



Neogene Kinematics of the Potwar Plateau and the Salt Range, NW Himalayan Front: A Paleostress Inversion and AMS study

Abdul Qayyum, Jorik Willem Poessé, Nuretdin Kaymakci, Cornelis G. Langereis, Erhan Gülyüz & Naveed Ahsan

To cite this article: Abdul Qayyum, Jorik Willem Poessé, Nuretdin Kaymakci, Cornelis G. Langereis, Erhan Gülyüz & Naveed Ahsan (2021): Neogene Kinematics of the Potwar Plateau and the Salt Range, NW Himalayan Front: A Paleostress Inversion and AMS study, International Geology Review, DOI: [10.1080/00206814.2021.1929514](https://doi.org/10.1080/00206814.2021.1929514)

To link to this article: <https://doi.org/10.1080/00206814.2021.1929514>



© 2021 The Author(s). Published by Informa UK Limited, trading as Taylor & Francis Group.



[View supplementary material](#)



Published online: 27 Jun 2021.



[Submit your article to this journal](#)



Article views: 1048








[View related articles](#)



[View Crossmark data](#)

Neogene Kinematics of the Potwar Plateau and the Salt Range, NW Himalayan Front: A Paleostress Inversion and AMS study

Abdul Qayyum ^{a,b}, Jorik Willem Poessé^b, Nuretdin Kaymakci ^a, Cornelis G. Langereis ^b, Erhan Gülyüz ^c and Naveed Ahsan ^d

^aDepartment of Geological Engineering, Middle East Technical University (METU/ODTÜ), Ankara, Turkey; ^bDepartment of Earth Sciences, Utrecht University, 3584 CB Utrecht, The Netherlands; ^cDepartment of Geological Engineering, Van Yüzüncü Yıl University, Van, Turkey; ^dInstitute of Geology, University of the Punjab, Lahore, Pakistan

ABSTRACT

We provide new kinematic data from the Potwar Plateau (Pakistan) to evaluate the tectonic evolution of the region during the Neogene. The plateau is bound by two major strike-slip faults in the west and the east, accommodating its southwards translation.

We have recognized two Neogene deformation phases in the plateau, based on paleostress inversion and Anisotropy of Magnetic Susceptibility (AMS) tensors. The first phase lasted until the early Pliocene and was characterized by vertical minor stress and N-S compression, implying thrust tectonics. The second deformation phase is characterized by a near-vertical intermediate principal stress and near-horizontal major and minor stresses, interpreted to be associated with strike-slip tectonics since the late Pliocene.

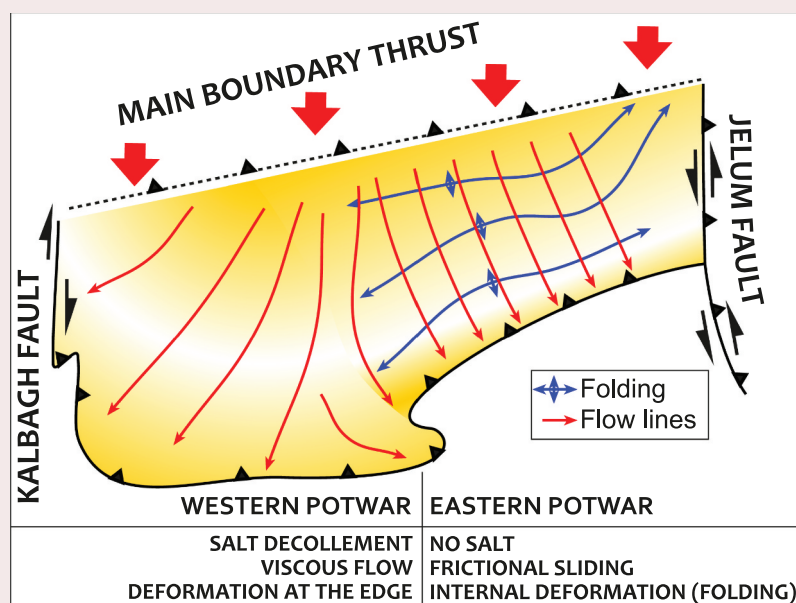
K_{int} vectors from 21 sites are relatively compatible with the major principal stress orientations (σ_1) and indicate two distinct domains. This is possibly because K_{min} orientations are related to compaction, whereas K_{int} orientations were always parallel to tectonic shortening and hence compression direction during both strike-slip (post-late Pliocene) and thrusting (pre-late Pliocene) phases. These phases are characterized by swapping of (σ_2) and (σ_3) orientations while (σ_1) maintained its orientation. The most prominent change occurs at the western part of the Potwar Plateau, where major principal stress directions (σ_1) and K_{int} axes fan out south-westwards. The eastern domain is dominated by NE-SW trending folds and thrust faults, which are absent in the western domain. These structural features are interpreted to be the result of the distribution of deposits of the Neoproterozoic Salt Range Formation as a substratum below the Potwar Plateau. The Salt Range Formation is very thick and widespread in the west area and almost absent in the east. This factor led to unconstrained southwards gliding of the Potwar Plateau over the salt deposits in the west as opposed to frictional sliding and substantial internal deformation in the east.

ARTICLE HISTORY


Received 15 February 2021
Accepted 8 May 2021

KEYWORDS

Kinematics; paleostress inversion; Anisotropy of Magnetic Susceptibility (AMS); potwar plateau; salt range



CONTACT Abdul Qayyum  a.qayyum@uu.nl, geologist.aqayyum@gmail.com  Middle East Technical University (METU/ODTÜ), Department of Geological Engineering, Ankara 06800, Turkey. Department of Earth Sciences, Utrecht University, 3584 CB Utrecht, The Netherlands

 Supplemental data for this article can be accessed [here](#)

© 2021 The Author(s). Published by Informa UK Limited, trading as Taylor & Francis Group.

This is an Open Access article distributed under the terms of the Creative Commons Attribution-NonCommercial-NoDerivatives License (<http://creativecommons.org/licenses/by-nc-nd/4.0/>), which permits non-commercial re-use, distribution, and reproduction in any medium, provided the original work is properly cited, and is not altered, transformed, or built upon in any way.

1. Introduction

The convergence between the Indian Plate and Eurasian plates is still ongoing and responsible for the main tectonic events in the Himalayas. The estimated inception of the India-Eurasian collision is about 50–60 Ma, which

took place after the closure and complete obliteration of the Neotethys oceanic lithosphere (DeCelles et al., 2002; Kapp and Decelles, 2019; Molnar and Tapponnier 1978; Meade 2007; Najman et al. 2010). At present, the Indian

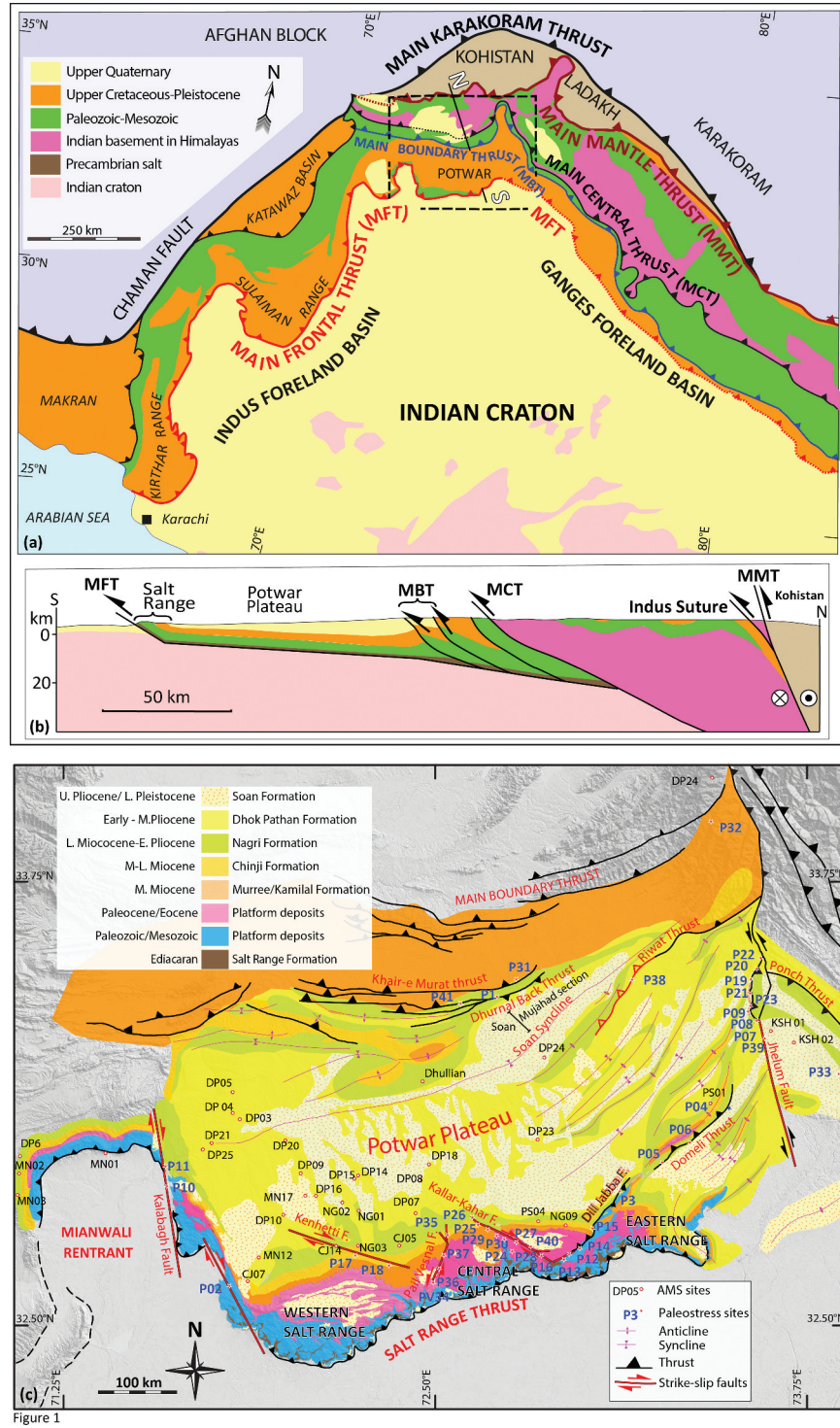


Figure 1. A) Major tectonic elements in the NW Himalayas (Butler 2018). b) Simplified cross-section along the line NS (redrawn from DiPietro and Pogue 2004). c) Geologic map of the Potwar Plateau and the Salt Range (Modified after Gee 1989) showing sampling site locations.

Plate has been deformed into numerous fold-thrust belts. These include the Sulaiman Range in the west and the Potwar Plateau in the NW (Figure 1). The Sulaiman Range is an east-verging fold-thrust belt delimited in the west by the Chaman Fault, a suture zone that separates the Indian Plate from the Eurasian Plate and demarcates the former position of the Neotethys. To the NW, the suture is marked by the Main Mantle Thrust (MMT) and is referred to as the Indus Suture Zone (Hodges 2000) (Figure 1(a, b)).

Foreland propagating sequences of thin-skinned thrust sheets and fold belts bounded by major faults are responsible for the compartmentalization of the Himalayas between the Indus Suture Zone (Main Mantle Thrust in Figure 1) – delimited in the south by the Main Mantle Thrust – and the Himalayan Frontal Thrust (MFT) (Figure 1). The Greater Himalayas are composed of rocks metamorphosed at about (30 Ma), volcanic and sedimentary rocks and are bounded by the Indus suture in the north (MMT) and by the Main Central Thrust (MCT) in the south (Chaudhry and Ghazanfar 1990; DiPietro and Pogue 2004). The Lesser Himalayas are composed of Proterozoic metamorphosed rocks overlain by sedimentary rocks, of which the youngest marine deposits are of Eocene-Oligocene age (DiPietro and Pogue 2004).

The Lesser Himalayas are bounded by the Main Central Thrust (MCT) in the north and by the Main Boundary Thrust (MBT) in the south (Tapponnier *et al.* 1986; DiPietro and Pogue 2004).

A continental foreland fold-thrust belt known as the Potwar Plateau and the Salt Range, developed between the Main Boundary Thrust (MBT) in the north and the Main Frontal Thrust (MFT) in the south (Lillie 1987; McDougall *et al.* 1993), respectively (Figure 1c). The Foreland Basin (Potwar Plateau) mainly consists of Neogene sedimentary rocks, named as the Siwaliks Group. These strata are associated with Himalayan deformation front propagation southwards into the Potwar Plateau and the Salt Range, which recorded all the major deformation phases related to the development of the Himalayan frontal foreland basin during the Neogene (Baker *et al.* 1988; Yeats and Thakur 2008). However, there have been no comprehensive studies done to determine the kinematics of the region, which is necessary to resolve the different stages of deformation at the Himalayan front.

This paper attempts to unravel the Neogene deformation history of the NW Himalayan deformation front using newly obtained kinematic data based on fault slip data sets and AMS data collected from Siwaliks Group rocks exposed in the Potwar Plateau and the Salt Range. For this purpose, we integrated the results of paleostress

inversion with AMS vectors, which typically correspond to major strain axes in slightly to mildly deformed sedimentary rocks (Hirt *et al.* 1993; Sagnotti and Speranza 1993; Henry 1997; Borradaile 2001; Pares and Van Der 2002). This is also the case for the Potwar Plateau, which is mildly deformed as indicated by the broad and gentle folding, and it lacks major internal strike-slip displacement. Therefore, the orientations of the stress and strain axes are expected to exhibit correlation in the region.

1.1. Geologic Setting

The study area comprises the Potwar Plateau and the Salt Range in NW Pakistan, developed at the NW deformation front of Himalayan orogen (Figure 1). The Potwar Plateau is a fold and thrust belt and is delimited in the north by the Main Boundary Thrust Belt, the Kalabagh Fault in the west, the Jhelum Fault in the east, and the Salt Range in the south (Ahmad Abir *et al.* 2015). The Kalabagh Fault is a dextral strike-slip fault developed as an accommodation structure at the western margin of the Potwar Fold-Thrust Belt. It is a lateral ramp structure developed due to the southwards movement and internal deformation of the Potwar Plateau sedimentary wedge (Khan *et al.* 2012; Qayyum *et al.* 2015). The eastern boundary of the Potwar Plateau is less well defined compared to the western margin. This is possibly due to the uninterrupted deposition of Siwaliks strata both in the eastern and western sides of the sinistral Jhelum Fault, which obscured the development of a through-going single fault zone (Pennock *et al.* 1989; Grelaud *et al.* 2002). As a result, the southwards propagating deformation front gave way to the development of a sedimentary wedge in the Potwar Plateau, where thicker accumulations are found in the north and thinner in the southern margin. Similarly, southwards thrusting of the Neoproterozoic Salt Range Formation possibly stopped at a normal basement fault at the core of the Salt Range, resulting in the development of the Salt Range and salt avalanches in front of the range, along the Salt Range Thrust (Davis and Engelder 1985).

The stratigraphy of the region is represented by Miocene to Quaternary sedimentary deposits with one regional unconformity at the base of the Upper Pliocene section (Gee 1989) (Figure 2). These units consist of Rawalpindi and Siwaliks Groups (Yeats *et al.* 1992). The movement of allochthonous salt in the region is responsible for developing out-of-sequence thrusting and reactivation of the pre-existing faults in the Potwar Plateau and the Salt Range (Grelaud *et al.* 2002). Therefore, structures related to the salt displacement are of key importance to understand the structural development in the Potwar Plateau and the Salt Range, which remains

tectonically active based on the recent seismic activity and GPS velocities (Jadoon et al., 2014; Yeats et al. 1984; Jouanne 2014).

The Northern Potwar Deformed Zone (NPDZ) is associated with the footwall deformation of the Main Boundary Thrust. However, the structural styles in NPDZ are somewhat different in comparison to the rest of the Potwar Plateau. Based on deformation styles, the Potwar Plateau can be divided into two domains, the eastern and western Potwar Plateau. The eastern Potwar Plateau is dominated by fault propagation fold type structures (Pennock et al. 1989) and the western plateau is dominated by fault bend fold structures (Qayyum et al. 2015). The Potwar Plateau is bounded to the south by the Salt Range Thrust of the Himalayan Frontal Thrust system.

Neogene strata are the main focus of this study, and therefore, pre-Neogene rocks are designated as the underlying 'basement'. The oldest sedimentary unit in the region is the Eo-Cambrian Salt Range Formation, consisting of shale and evaporite rocks exposed along the eastern segment of the Salt Range Thrust. Cambrian strata of the Jhelum Group overlie this formation, and the evaporate levels of the unit acted as decollement horizons in the region (Yeats et al. 1984). These rocks are overlain by Lower Permian strata, represented by Gondwana glacio-fluvial deposits of the Tobra Formation. They are overlain by detrital strata of Nilawahan Group. The Late Permian is represented by the Zaluch Group, mainly containing carbonate facies rocks intercalated with detrital rocks. Triassic is represented largely by the detrital facies, and the late Triassic is represented by the limestone of the Kingriali Formation. Overlying Jurassic strata are dominated by detrital rocks at the base called the Baroch Group and mainly limestone at the top (Suleiman Group). Cretaceous strata include detrital rocks of the Surgher Group. The Palaeocene Makarwal Group is represented by the detrital rocks at the base and Lockhart Limestone in the middle, and shales of the Patala Formation at the top. Eocene strata are dominated by the limestones and shales of the Charat Group. These Eocene strata represent the youngest marine deposits in the Potwar Plateau and the Salt Range (Lillie 1987; Gee 1989).

1.2. Neogene stratigraphy of potwar plateau

Neogene sequences in the Potwar Plateau comprise continental deposits accumulated during the late-stage rise of the Himalayas (Gee 1989). The Lower Miocene sequences comprise the Rawalpindi Group and represent the earliest continental deposits, which unconformably cover Eocene marine strata in the region (Figure 2).

The Rawalpindi Group includes the Murree and Kamliyal formations (Baker et al. 1988; Gee 1989).

The Murree Formation is represented by purple grey and greenish-grey sandstone intercalated with some intra-formational conglomerates. The base of the formation contains conglomerates with abundant clasts of reworked rocks with Eocene foraminifera. These conglomerate levels are interpreted as the basal conglomerates. The Kamliyal Formation overlies the Murree Formation conformably. It is distinguished easily in the field by purple to greenish-grey and dark brick-red sandstone layers intercalated with purple shales. The age of the Kamliyal Formation is regarded as Middle to Late Miocene (Gee 1989).

Rawalpindi Group strata are overlain by the Siwalik Group, which consists of Himalayan molasses sequences. These rocks are widely distributed in the Sub Himalayas (e.g. Indus basin and the northwest margin of the Indian continent). The Siwaliks Group sequence is divided into two Lower and Upper Siwaliks, separated by a regional unconformity. The Lower Siwaliks contains Chinji, Nagri, Dhok Pathan formations, and the Upper Siwaliks, represented by the Soan Formation and Lei Conglomerate (Gee 1989). The Chinji Formation consists of red claystone interbedded with fine to medium-grained sandstone layers. This unit is widely exposed throughout the Potwar Plateau. The depositional age for the formation is assigned as Late Miocene (Gee 1989). It has a conformable contact with the overlying Nagri Formation, which consists of greenish-grey medium to coarse-grained sandstone layers with some subordinate claystone intervals. The age of this formation is late Miocene to early Pliocene (Yeats and Hussain 1987; Baker et al. 1988; Gee 1989; Tauxe and Feakins 2020). The Nagri Formation is conformably overlain by the Dhok Pathan Formation, the uppermost unit of the Lower Siwaliks. The Dhok Pathan Formation consists of alternating sandstone and shale layers and intercalations of conglomerates. It is widely exposed in the Potwar Plateau along the Soan River and the Salt Range and Early to Middle Pliocene age is assigned to the formation (Gee 1989). The strata of the Upper Siwaliks Group unconformably overlie this unit. The Soan Formation is the lower member of the Upper Siwaliks Group. It consists of conglomerate, sandstone, and claystone layers. The Soan Formation is disconformably underlain by the Dhok Pathan Formation, and it has an angular contact with the overlying Lei Conglomerate. The age of the Soan Formation is assigned as Late Pliocene to Early Pleistocene (Astian to Villafranchian) (Opdyke and Lindsay 1979). The Lei and Kalabagh conglomerates are composed of fluvial outwash sequences

QUATER.	HOLOCENE		Alluvium	Various alluvial clastics	SAMPLED HORIZONS
	PLEISTOCENE	Upper Siwaliks	Lei/Kalabagh	Mainly conglomerates	
Soan			Sandstone, shale, conglomerate alternation		
NEOGENE	PLIOCENE	Lower Siwaliks	Dhok Pathan	Sandstone, conglomerate alternation	
			Nagri	Sandstone, shale alternation	
	MIOCENE	Rawalpindi	Chinji	Shale intercalated with sandstones	
			Kamlial	Greenish grey sandstone	
			Murree	Red sandy mudstone	
OLIGOCENE					
EOCENE	Charat		Kuldana	Shallow marine limestone, marl and nodular limestone intercalations	
			Chorgali		
			Sakesar		
			Nammal		
PALEOCENE	Makarwal		Patala	Dark gray, organic-rich shale, marl intercalated with massive nodular limestone, pisolitic sandstone.	
			Lockhart		
			Hangu		
CRETACEOUS	Surgher		Lumshiwali	EROSION Sandstone, shale, marl, limestone	
			Chichali		
JURASSIC	Suleiman	Baroch	Samana Suk	EROSION Limestone, sandstone, siltstone, shale	
			Shinawri		
			Datta		
TRIASSIC	Musa Khel		Kingriali	Shale, limestone, marl, mudstone intercalations	
			Tredian		
			Mianwali		
PERMIAN	Zaluch	Nilawahana	Chhidru	UNCONFORMITY Sandstone, limestone, shale, marl intercalation and conglomerates at the base.	
			Wargal		
			Amb		
			Sardhi		
			Tobra		
ORDOVICIAN-CARBONIFEROUS				Glacial deposits	
CAMBRIAN	Jhelum		Baghanwala	EROSION	
			Jutana Kussak Khewra		
EDIACARAN				Intercalation of evaporites, red shale and sandstone	
			Salt Range		

Figure 2. Lithostratigraphic units exposed in and around the Potwar Plateau and the Salt Range (Modified from Gee 1989; Tauxe and Feakins 2020).

containing reworked clasts with minor sandstone layers. The age of these deposits is assigned as Pleistocene. All the rocks in the study area are locally unconformably overlain by Quaternary alluvial deposits (Figure 2).

2. Methods

This study is based mainly on field data collection and analysis. It includes remote sensing studies, including observation and analysis of major structures in the

field, and fault slip data collection. The last stage includes data collection for AMS measurements and analysis. To evaluate major structures in the region, available satellite images, including Landsat TM, ETM+, Digital Globe images, are processed and interpreted with the help of published geologic maps by the Geological Survey of Pakistan (Gee 1989). A rigorous field study was then conducted in three field seasons (2015, 2016, and 2017). During the field studies, previously identified structures are studied in detail, and from most of the faults encountered in the field, fault slip data have been collected wherever kinematic indicators on the fault planes are exposed and preserved. During these studies, AMS sampling from Neogene strata was also performed.

2.1. Paleostress inversion

Fault-slip data of a brittle nature have often been used to reconstruct the orientation of principal stress axes (Etchecopar *et al.* 1981; Angelier 1984). So far, several methods have been developed for paleostress inversion and the reconstruction of paleostress tensors (Angelier 1994, 1984, 1979; Armijo *et al.* 1982; Carey-Gailhardis and Mercier 1987; Etchecopar *et al.* 1981; Fleischmann and Nemcok 1991; Gephart 1990; Gephart and Forsyth 1984; Kenneth C. Hardcastle 1989; Marrett and Allmendinger 1990; Nieto-Samaniego and Alaniz-Alvarez 1997; Reches 1987; Will and Powell 1991; Yin and Ranalli, 1993). For multiphase deformation and mixed fault slip data, various separation algorithms have been proposed over the last three decades (e.g. Hardcastle and Hills 1991; Krantz 1988; Liesa and Lisle 2004; Žalohar and Vrabec 2007). However, the best separation approach for multiphase data must be based on observation, and meticulous examination of the fault slip data in the field (Angelier 1994; Lisle, 2004). Slip directions are generally deduced from the orientation of slickenlines, such as slickensides, frictional grooves or fibrous mineral growth patterns (slickenfibers) (Fleuty, 1974; Doblás 1998). Methods used in the paleostress analysis are based upon the assumption that slip occurs along with the maximum resolved shear stress, which is also presumed to be aligned with the slickenside direction (Wallace 1951; Bott 1959; Aleksandrowaski 1985). Slip direction on a fault can also be inferred utilizing the focal mechanism solution of earthquakes (Angelier 1984; Gephart and Forsyth 1984; Carey-Gailhardis and Mercier 1987) and by the orientation of calcite deformation twins (Lacombe 2010). Additionally, most studies assume that a single tectonic event is marked by a single regional homogeneous stress field. This suggests that a single stress

deviator develops a slip direction on a fault plane, and all the faults that are displaced during a single tectonic event are displaced separately in such a way that it is conformable with a single-stress deviator (Will and Powell 1991).

In this study, Win_Tensor V5.8.8 software developed by Delvaux and Sperner (2003) is used to construct paleostress configurations for each site. For the analysis of each data set, the R-Optimized routine is used. During the analysis, the maximum misfit angle is selected to be 30° (Delvaux and Sperner 2003). The data that do not meet this criterion are excluded from paleostress analysis and are classified as spurious. The total number of spurious data are found to be 26, which makes up only 1.8% of the entire data set.

2.1.1 Paleostress sampling

More than 1400 fault slip measurements from 41 discrete sites in the Potwar Plateau and the Salt Range were collected (Figure 1b). For each data set, fault plane attitude, rakes of slickensides, and movement senses are recorded (Figure 3). For relative age determination of the kinematic events, the host rock types of these structures are also recorded in the field. Overprinting slickensides, or contrasting kinematic indicators within the same fault plane, which might be related to different deformation phases, are noted and recorded separately. However, such field relations were rare and occurred only at two sites (P2 and P41). The stratigraphic foot-wall/hanging wall relationships of the faults were determined, and stratigraphic offset magnitudes along the faults are also measured.

The sampling at a site was performed according to techniques outlined in Kaymakci *et al.* (2000), which requires that all data from a site must be kept within a 50 m diameter in order to maintain structural homogeneity (Hancock 1985). The faults with more than 20 m displacement are separated and are analysed separately (e.g. one site along the Kallar–Kahar Fault), because they could accommodate large strain such that paleostress and strain axes may not be parallel due to non-coaxial deformation. Therefore, the site-based data collected in relation to large structures belong only to the youngest stratigraphic unit that they displaced. The obtained stress configurations are tabulated in Supplement 1 and depicted in Supplements 2. The analysis of the combined paleostress orientations is presented in Figure 4.

2.2 Anisotropy of Magnetic Susceptibility (AMS)

The AMS technique is based on the measurement of the low-field magnetic susceptibility (K), which describes the

linear relation between the magnetic field (H) and the induced magnetization (M) of the sample as determined using the formula $M = kH$ (Jelínek 1978; Jelínek 1981; Hrouda 1982). AMS data have been widely used to evaluate the rock fabric in structural geology, tectonics, and sedimentology (Hrouda 1982; Jackson and Tauxe 1991; Rochette *et al.* 1992; Borradaile and Henry 1997; Borradaile 2001; Borradaile and Jackson 2004). The AMS approach is a non-destructive and relatively fast method for rock fabric analysis compared to the more complex and time-consuming techniques like X-ray goniometry and neutron goniometry. Mathematically,

The AMS is described by a second-degree tensor with direction and magnitudes, reflecting the directional variance of magnetic susceptibility. The utility of the AMS technique in strain determinations has been shown by Hrouda and Janak (1976) and Lee and Angelier (2000).

The susceptibility tensors consist of principal susceptibilities ($K_1 \geq K_2 \geq K_3$; $K_{\max} > K_{\text{int}} > K_{\text{min}}$). During deformation, the maximum axis of the susceptibility vector (K_{\max}) tends to be parallel to the maximum extension direction (stretching direction), while the minimum axis of susceptibility (K_{\min}) is typically parallel to the compaction direction in low to mildly deformed rocks (Duermeijer *et al.*

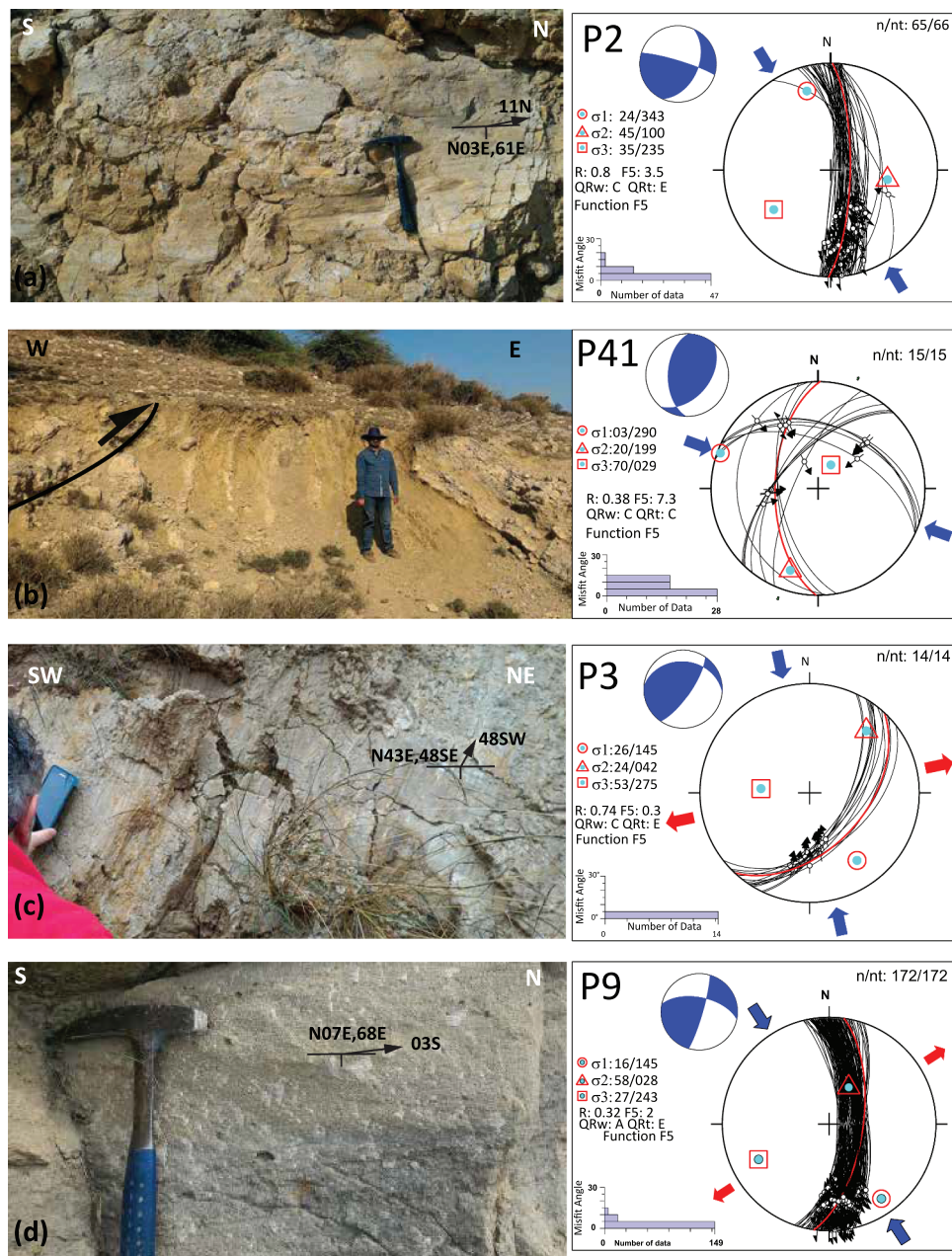


Figure 3. Field pictures of exposed faults encountered during field studies and constructed paleostress configurations (a-d). Arrows indicate the motion of the hanging-wall block.

1998). The remaining third axis (intermediate axis, K_{int}) of the susceptibility tensor tends to be parallel to the major principal stress axis in low to mildly deformed sedimentary rocks (Jelinek 1981; Jelínek 1978). In other words, depending on the tectonic setting, the intermediate axis (K_{int}) might be parallel to the main tectonic compression direction. However, major compression corresponds to the vertical stress in extensional settings, so that K_{min} and shortening directions might be parallel. Therefore, the intermediate susceptibility axis (K_{int}) may be parallel to the intermediate principal stress direction, provided that no simple shear or rotational deformation is involved in the deformation of rocks (Means 1976; Aubourg *et al.* 1990). Most of the AMS measurements are performed on rocks from sites exposed in the central part of the Potwar Plateau, where a few faults are exposed (Figure 1).

2.2.1 AMS sampling and measurement

Relatively undeformed strata in the Potwar Plateau are sampled for AMS studies, and sampling locations are chosen based on the availability of accessible outcrops suitable for sampling. Moreover, fine-grained sediments, including mainly red massive mudstones, grey to greenish-grey mudstones, and occasionally marls, were preferred as these are deposited in a relatively low-energy environment. A total of 176 oriented cores were collected from Neogene rocks at 23 sites using handheld electric-powered drilling equipment. For each sample, drilling orientations and bedding attitudes were recorded. In addition, stratigraphic ages of AMS samples were determined in the field with the help of stratigraphy and geologic maps.

The diameter of the core samples is 25 mm, and these were cut into separate conventional specimens using a dual blade rock saw, and standard specimen

size (of 22 mm height) is maintained for the AMS samples. The unused parts of the large samples are kept for further analyses. The same samples are used for palaeomagnetic and rock magnetic purposes (not reported here). Prior to palaeomagnetic analysis, each specimen is measured for its magnetic anisotropy (AMS). In order to obtain accurate results, only unbroken, crack-free, and uniform shape specimens were measured because AMS results are very sensitive to the physical characteristics of the specimens. Each sample was measured on a Kappabridge, which measures the AMS of a spinning specimen fixed in the rotator, and the results are averaged to obtain the AMS tensor described by three principal axes ($K_1 = K_{max}$, $K_2 = K_{int}$, and $K_3 = K_{min}$). Measurements were performed using the multi-function Kappa bridge MFK1-FA (Agico, Czech Republic), an automated field variation (low field, 200 A/m) susceptometer (Studýnka *et al.* 2014). The measurement sensitivity of the instrument is 10^{-8} SI, which enables the measurement of sediments of low susceptibilities. Measurement and analysis were done at Fort Hoofddijk Palaeomagnetic Laboratory of Utrecht University (The Netherlands). The measurements were then interpreted using Anisoft 4.2 and Anisoft 5.0 softwares (Chadima & Jelinek, 2009). The resultant AMS fabric is then corrected for the bedding orientation. Mean directions of the principal axis of each site are estimated using Jelinek statistics (Jelínek 1978).

3. Results

3.1 Fault kinematics and paleostress analysis

The major faults controlling the deformation of the Potwar Plateau are the Salt Range Thrust (SRT), the

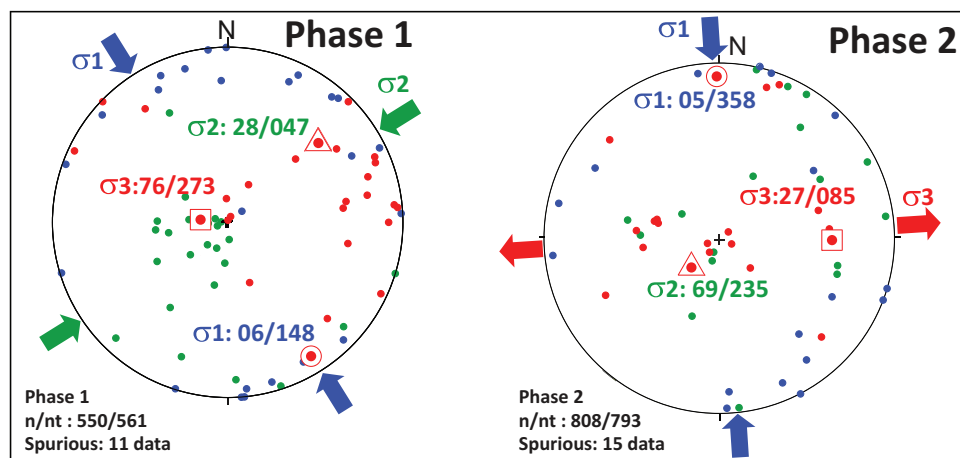


Figure 4. Equal area projections of paleostress orientations for deformation phases 1 and 2. n/nt: the number used vs measured fault slip data in the field. See Supplement 1 for the explanations of the text in the figures. (lower hemisphere, equal-area projection).

Kalabagh Fault, and the Jhelum Fault (Figure 1). In addition, in the southern part of the plateau, two conjugate sets of strike-slip faults have been dominant. These are Kenhetti (NW-SE) and Pail Vesnal (NE-SW) faults, and the other conjugate set is the Kallar-Kahar (NW-SE) and Krangal-Dill Jabba (NE-SW) faults.

The most prominent structure in the region is the Salt Range Thrust. It constitutes a part of the Main Frontal Thrust (MFT) of Indian-Eurasian convergence and along the Salt Range Thrust, Mesozoic to Ediacaran rocks (Figure 2) thrust over the Quaternary alluvial deposits on the Indian Craton (Figures 1 and Figures 5). This relationship indicates the young activity of the Salt Range Thrust. In addition to this prominent structure, several major thrust faults are also developed, mainly in the northern and easternmost margin of the Potwar Plateau. The most important of them include the Main Boundary Thrust, which juxtaposes Mesozoic and older rocks over Cenozoic strata, including Siwalik Group rocks. At the northern margin of the Potwar Plateau, south of the Main Boundary Thrust, along the Khair-e Murat Thrust, pre-late Miocene rocks are thrust over younger deposits. The East Ponch Thrust is a back-thrust along which upper Miocene strata are thrust over upper Pliocene and younger deposits. The youngest units deformed by these faults include Early Pliocene rocks. They are overlain unconformably by strata of the broadly folded Soan Formation of late Pliocene to Pleistocene age. This relationship indicates two different deformation phases that affected the region during the Neogene. The first phase lasted until the late Pliocene and was sealed by Soan Formation strata. However, the Soan Formation strata are also deformed and expressed by broad folds, mainly in the eastern half of the Potwar Plateau. Some folds are displaced by small-scale faults, especially in the north, close to the Khair-e Murat Thrust belt. These small faults are not more than a few kilometres in true length. Nevertheless, folding and faulting of Soan Formation strata indicate a younger deformation phase that took place after the deposition of the Soan Formation in the Late Pliocene and is possibly still active at present.

Two distinctive sets of paleostress configurations characterize the region. These include sites with strike-slip solutions associated with strike-slip faults in the western margin of the Potwar Plateau, such as the Kalabagh Fault and the Salt Range thrust. The Kenhetti, Kallar-Kahar, Pail-Vesnal, and Dill-Jabba faults are associated with the development of the Salt Range, and the sites along these faults produced mostly transpressional paleostress solutions. Other strike-slip solutions are associated with the Riwat Thrust (site P38 in Figure 5), and the northern extent of the Jhelum Fault (sites P7-9) and

also along the western extent of the Riwat Fault (Figure 5). For most of these sites, the horizontal component of the major stress (σ_1) is almost N-S, while the minor stress is oriented E-W (Figure 5, Supplement 2).

Most of the contractional solutions, as expected, are associated with thrusts, and the orientation of the major principal stress (σ_1) varies according to the attitudes of associated thrust faults. However, these are almost always oblique to the local trend of the thrust faults. This relationship is interpreted to suggest that, except for a few locations, none of the thrust faults in the region is pure dip-slip faults, and they have lateral components in variable degrees.

As mentioned above, two different deformation phases are also recognized in the region based on cross-cutting and stratigraphic relationships. The paleostress configurations for the first phase indicate both strike-slip and contractional deformation (Supplement 2). The solutions indicate vertical (σ_3) (contractional deformation) close to the thrust faults (e.g. sites 1,31,41,33,32). However, almost all of the solutions around the Salt Range are strike-slip in character (Figure 5, Supplements 1 and 2).

Paleostress configurations for sites affected by the second phase of deformation indicate strike-slip deformation except for some of the sites in the northern part of the Jhelum fault (sites 19–22) and the sites along Domeli Thrust (Figure 5).

The resolved paleostress orientations are analysed using Fisher statistics to determine their dominant direction (Figure 4). The phase 1 results yielded the following orientations: σ_1 :06/148 N, σ_2 :28/047 N and σ_3 :76/273 N. Having σ_3 almost vertical and other principal stresses almost horizontal indicates compressional-contractional (thrust) tectonics. Similarly, the dominant principal stress orientations for phase 2 are as follows; σ_1 : 05/358 N, σ_2 :69/235 N and σ_3 :27/085 N. Having intermediate stress almost vertical and other principal stress almost horizontal indicates transcurrent (strike-slip, compressional-extensional) tectonics.

3.2 AMS results

One hundred seventy-six specimens from 23 sites were measured and analysed independently (Supplement 4). The specimens belonging to two or occasionally three adjacent sites (same geographic location and same age) were grouped into one locality so that N is sufficiently large to allow meaningful locality statistics. These locality means are tabulated in Supplement 3, depicted in Supplement 4. In addition, the mean susceptibility (K_m) histogram is depicted in Figure 6a. The k_m values show a wide range, from very low values to

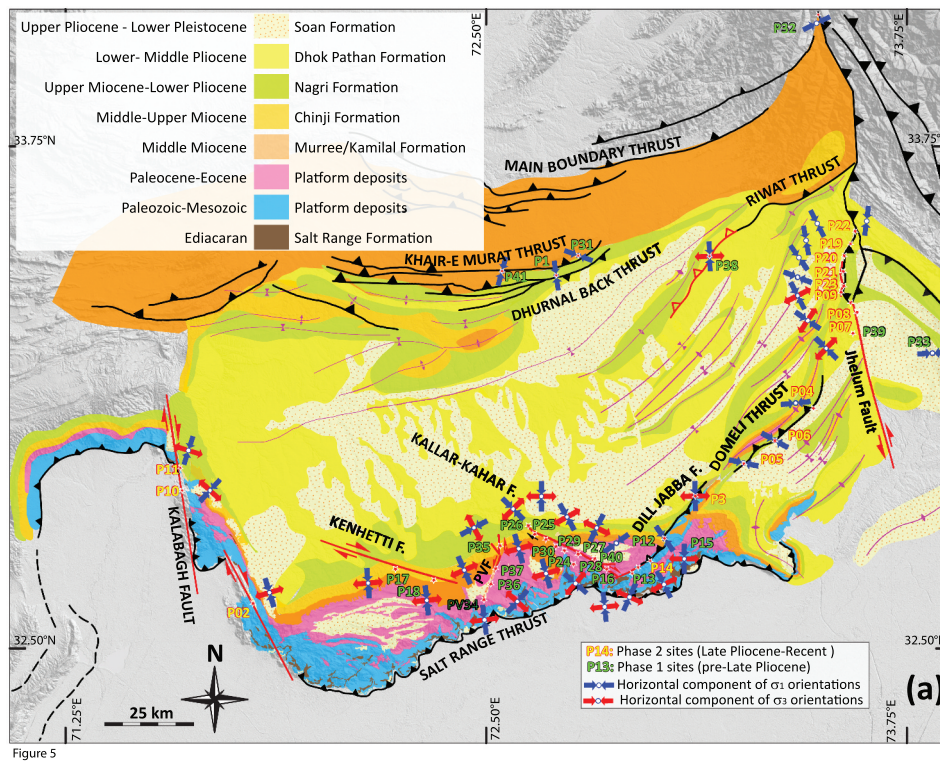


Figure 5

Figure 5. Major faults and horizontal components of major and minor principal stresses. Sites with both σ_1 and σ_3 arrows indicate strike-slip faulting, while sites with only σ_1 arrow indicate thrust tectonics.

values above 2000×10^{-6} SI (mostly ferromagnetic minerals). They are clustered around two main groups; the first one range between $200\text{--}1000 \times 10^{-6}$, and the second one ranges between $1200\text{--}2000 \times 10^{-6}$ SI). The variation in k_m is interpreted to be due to differences in the source (provenance) rocks and their constituent mineralogy. Relative foliation $F(K_{int}/K_{min})$ exhibits a wide range of distribution from $1.0 \leq F \leq 1.12$ ($F_{mean} = 1.0298$), as compared with lineation $L(K_{max}/K_{int})$ $1.0 \leq L \leq 1.026$ ($L_{mean} = 1.0064$). The F_{mean} is significantly higher than L_{mean} , as the majority of the foliation values are higher than lineation, reflecting the mainly oblate character of the distributions (Figure 6).

The corrected anisotropy degree P_j (Jelinek 1981) has a generally relatively low value ($P_j > 1.004$) with a mean of $P_j = 1.039$. In general, the AMS ellipsoids are oblate, but some have negative T values (prolate) in the data distribution. The correlation between T and P_j is very low, as indicated by no linear relationship between T and P_j , suggesting that the primary sedimentary structures (depositional anisotropy) play a negligible role. In addition, it also indicates that K_{max} and K_{int} are related to tectonic deformation while K_{min} is related to compaction; hence, the reliability of the AMS results for tectonic interpretation.

4. Discussion

4.1 Interpretation of paleostress data

Late Pliocene to Quaternary strata covers a large part of the study area. These deposits seal most of the older structures in the Potwar Plateau. In addition, the number of faults that offset the upper Pliocene to Quaternary are very scarce. This observation limits the possibility of systematic sampling of fault slip data in the region. However, such a limitation is partially overcome by interpolating the orientations of the horizontal component of the major stress axis (σ_1) over the study area to obtain regularly spaced σ_1 orientations. Because σ_2 is perpendicular to σ_1 and σ_3 is almost vertical at all sites, they are not interpolated. Although various interpolation techniques are available, we preferred the triangulation with linear interpolation technique in all our analyses because it is simple and straightforward. Since the distance between most sampling sites is larger than 10 km, and because of the large size of the study area, the grid size is taken as a quarter of a degree ($15''$, 0.25°), roughly corresponding to about 27.5 km. The sites belonging to phase 1 and phase 2 are analysed separately because their paleostress configurations are not coaxial (Figure 7).

The interpolated σ_1 orientations for phase 1 indicate σ_1 directions changing from NNE-SSW in the western

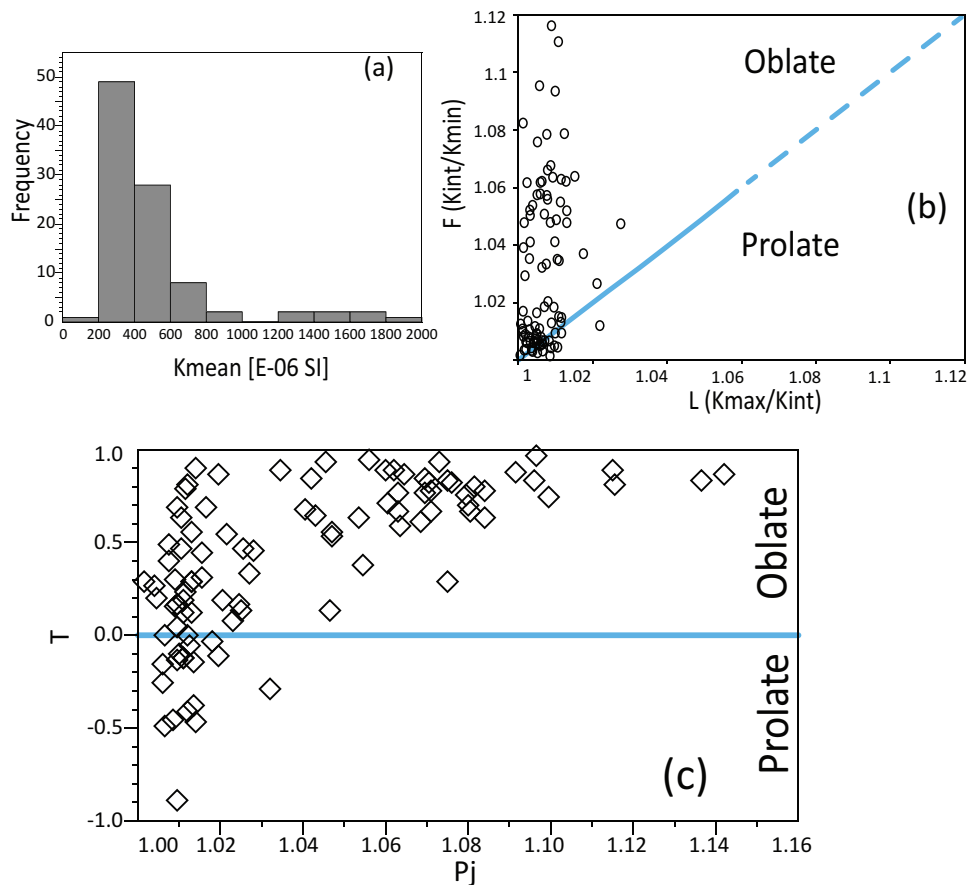


Figure 6. (a) Mean susceptibility histogram, (b) Lineation L (K_{\max}/K_{int}) versus Foliation F ($K_{\text{int}}/K_{\text{min}}$) Plot, (c) Pj (corrected anisotropic degree) versus T (Prolate/Oblate) plot (Shape factor).

margin of the Potwar plateau to N-S in the eastern part. However, slight anomalies are also present, especially in the central and eastern part of the plateau. Large variations are present mainly within the Salt Range and SE part of the plateau. Except for the northern part of the plateau, σ_1 directions are generally oblique to the major folds and faults in the study area. Considering near-vertical σ_3 and that of thrust-related deformation occurred during phase 1, it is safe to assume that the Potwar Plateau translated southwards and deformed orthogonally. However, such a uniform (like laminar flow) deformation style is disrupted at the leading edge of the plateau (resulting turbulent behaviour). Given the fact that the substratum consists of Ediacaran salt deposits, most of the plateau was likely translated passively southwards as a coherent but internally deformable semi-rigid block, and we infer that the main deformation took place at the leading edge around the Salt Range. During this phase of deformation and translation, the Kalabagh and Jhelum faults acted as lateral ramps.

Interpolated σ_1 orientations for phase 2 have a very discordant distribution. They are oriented almost N-S in the north near the Khair-e Murat Thrust but fan out from north-to-south in the west. Such a fanning out pattern is absent in the east. The orientations around the Jhelum Fault are oblique to the main trend of the fault, and they indicate the sinistral nature of the Jhelum fault. The orientations around the Domeli thrust are different in the hanging-wall and footwall-block of the thrust. It is obvious from the map (Figure 7b) that the thrust fault acts as a stress discontinuity where the orientations in the north are relatively uniform while they become chaotic in the south, on the footwall blocks.

The overall stress orientations associated with phase 2 deformation imply that to the north of Salt Range, Dill Jibba, and Domeli thrusts, the Potwar Plateau is detached from the underlying substratum and is translated over the Ediacaran Salt sequence, sliding southwards under the influence of gravity like a giant gravity-driven, relatively consistent thick viscous fluid (Borderie *et al.* 2018).

4.2 Interpretation of AMS orientations

In relatively undeformed to mildly deformed sedimentary rocks, the AMS axes correspond to deformation axes in an area. However, assigning any AMS axis to a specific deformation axis depends on the tectonic regime. For example, in extensional systems, the K_{\max} axis typically corresponds to the extension direction while K_{\min}

corresponds to compaction (Jelínek 1978; Jelinek 1981; Duermeijer *et al.* 1998). However, in the case of intense contractional deformation regimes (edgewise compression), K_{\min} may also correspond to a major shortening direction. It is not the case in the Potwar Plateau. In such mildly deformed terranes, K_{\min} is usually normal to the bedding plane, and it is usually indicative of compaction rather than tectonic shortening. In such systems, K_{\max} is

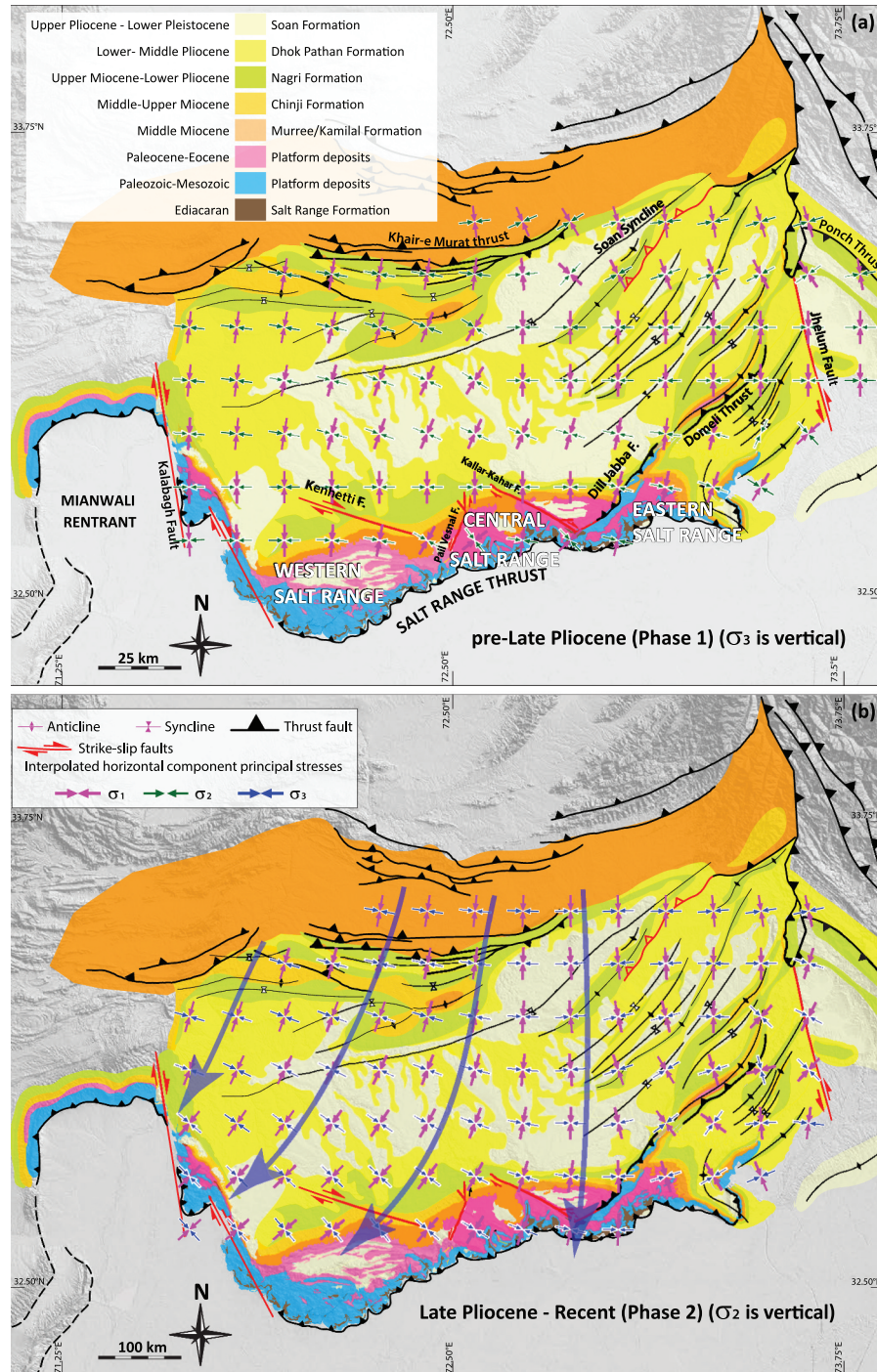


Figure 8

Figure 7. Interpolated horizontal components of principal stress orientations a) phase 1, b) phase 2 of deformation. Note fanning out of stress orientations for phase 2 (large blue arrows).

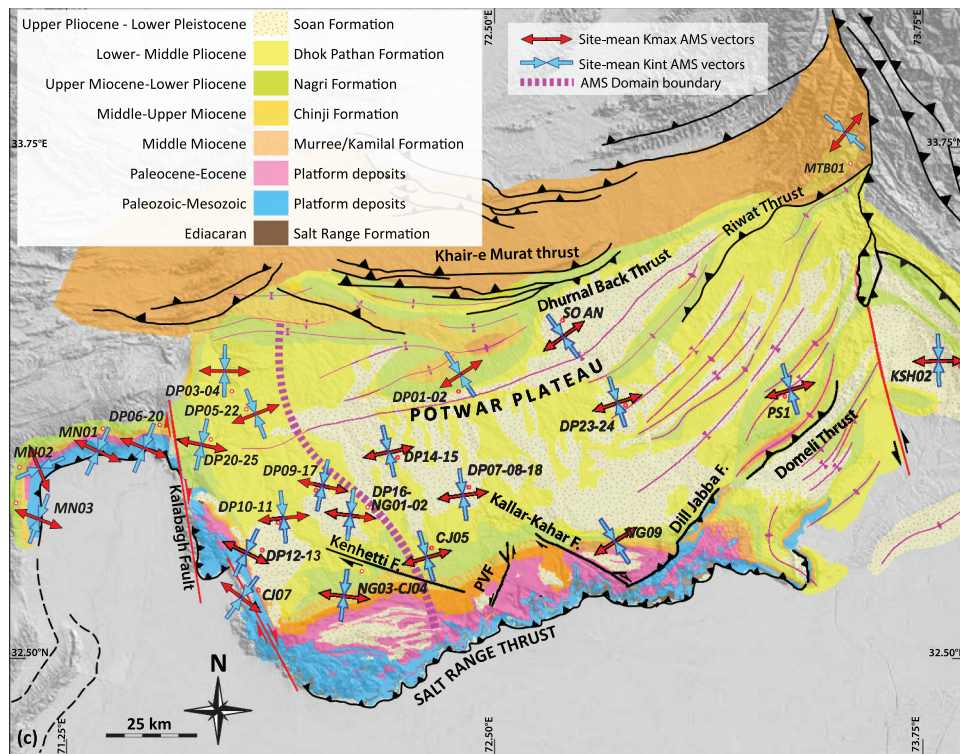


Figure 8. Map showing the horizontal components of the site mean K_{int} and K_{max} orientations after bedding tilt correction.

perpendicular to compression direction while K_{int} corresponds to the major compression direction. The mean values of K_{int} and K_{max} axes per site are depicted in Figure 8 to illustrate the dominant directions of shortening (K_{int}) and extension (K_{max}) in the Potwar Plateau. In order to display smoothed distribution, site-based K_{int} orientations are interpolated with a 15 arc minutes grid spacing. The results are illustrated in Figure 9.

The pattern of K_{int} orientations indicates two distinct domains (Figures 8 and Figures 9). In the western part of the Potwar Plateau, the K_{int} axes are oriented dominantly in the NNE-SSW direction while in the east. However, they are oriented NNW-SSE except for the easternmost site (KSH02), where they are oriented almost N-S. The western boundary of the western domain is defined by the right lateral Kalabagh Fault, while its eastern boundary is defined by a marked change in the orientations of the K_{int} in the domain, especially at CJ05 and DP14-15 sites from NE-SW to NW-SE orientation. The southern end of the domain boundary corresponds to Kenhetti Fault, and its northern end corresponds approximately to a relay zone of the western extension of Khair-e Murat Thrust (Figure 9).

4.3 Integration of paleostress and AMS results

In the case of pure shear or coaxial deformation (non-rotational deformation), principal stress and strain axes are colinear. This relationship can be tested simply by comparing the overall strain and stress axes locally and regionally. For this purpose, interpolated principal strain axes (K_{int}) and major paleostress axes for each phase are compared. Because of the sampling locations for AMS and paleostress inversion purposes are not located at the same sites, the comparison is performed on the interpolated results, which are placed on a common geographic position (Figure 10). Interpolation is performed on 15 arc minutes grid spacing for each data sets, which roughly corresponds to 15 km.

There is a better match between σ_1 orientation and K_{int} for phase 2 (younger phase) compared to phase 1 (older phase). The match is more common in the SW part of the Potwar Plateau compared to its northern and eastern parts (Figure 10). However, close to the Kalabagh Fault, the discrepancy between K_{int} and σ_1 orientations (for both phases) increases markedly. The largest discrepancies in the eastern part of the Potwar Plateau are observed close to the Jhelum fault.

For a regional compression, rose diagrams showing horizontal components of major stress and K_{int} indicate that (Figure 10(b-d)) the dominant σ_1 direction for phase 1 ranges around N05W, while they are N20E for phase 2.

The secondary dominant direction for phase 2 is about N80W, indicating a bimodal distribution of major principal stress orientations. Such a marked distribution seems to be not recorded for phase 1. On the other hand, the dominant direction of the K_{int} occurs in N15E directions. Interestingly, there is no bimodal distribution observable for K_{int} orientations.

Except for the Mujahad section (Soan site), almost all of the AMS data were collected from rocks of Late Miocene to Early Pliocene age. Similarly, deformation phase 1 is assumed to be of Late Miocene to Early Pliocene. On the other hand, deformation phase 2 is assumed as Late Pliocene to Recent. We expect that the σ_1 axes and K_{int} axes would match better compared to deformation phase 1 orientations because AMS values include a larger age range from Late Miocene to Pliocene while deformation 2 corresponds only to Late Pliocene to Recent. However, σ_1 orientations for phase 2 match better with the K_{int} orientations compared to phase 1 (Figure 9(b-d)). This relationship implies that the tectonic component to the AMS fabric was acquired largely during the Late Pliocene to Recent (phase 2). As indicated by rose diagrams, the consistent orientations of overall K_{int} indicate that no major rotational deformation took place during the Late Pliocene to Recent. However, the same 10° to 15° of rotations is possible in

considering the misfit between paleostress and K_{int} orientations.

4.4. Regional tectonic implications

The structural development of the Potwar Plateau and the Salt Range occurred in two different deformation phases. The first phase of deformation lasted until the Early Pliocene with an almost horizontal and N-S directed σ_1 and subvertical σ_3 . Interpolated σ_1 axes are almost parallel to each other, and they are almost perpendicular to the Salt Range and the thrust faults in the northern margin of the Potwar Plateau. This relationship, together with N-S directed σ_1 and near-vertical σ_3 , is interpreted as the indication of N-S shortening associated with the south directed translation of thrust faults such as Main Boundary Thrust (MBT) and Khair-e Murat Thrust and associated other thrust faults in the region from the north-to-south.

The second phase of deformation is commenced in the late Pliocene and is possibly continuing at present. Similarly, σ_1 was also horizontal during the second phase of deformation, and σ_2 was almost vertical, while σ_3 is horizontal and oriented E-W. The near-vertical σ_2 and sub-horizontal orientation of σ_1 and σ_3 imply the domination of transcurrent (transpressional strike-slip) deformation. The radially fanning out σ_1

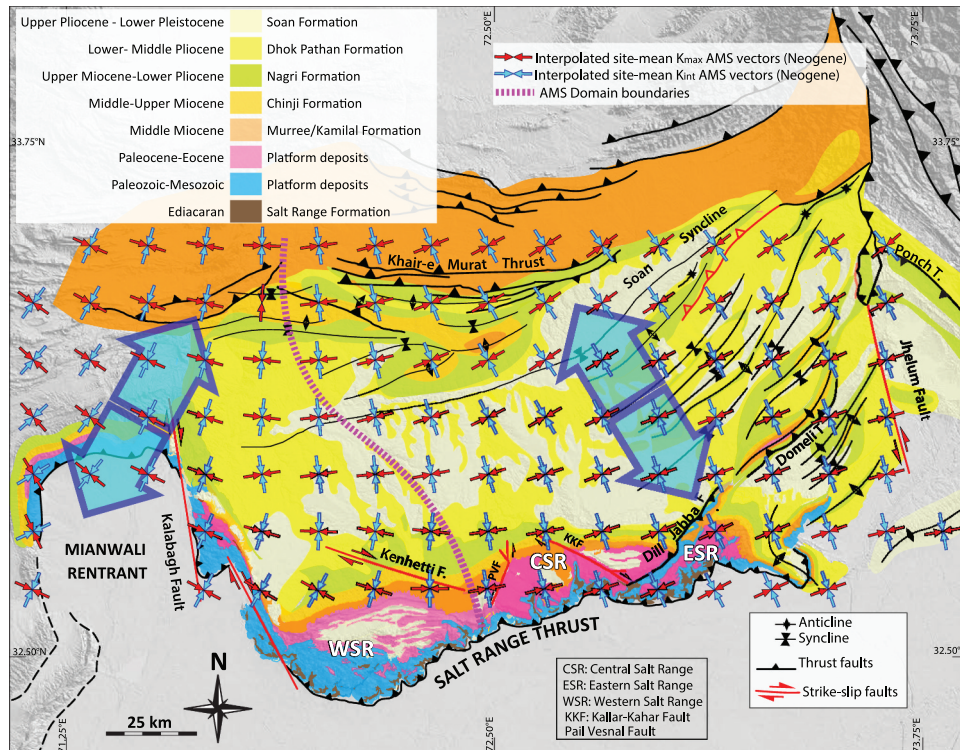


Figure 9. Interpolated K_{int} axes and AMS domain boundaries. Large blue faint arrows indicate dominant K_{int} directions.

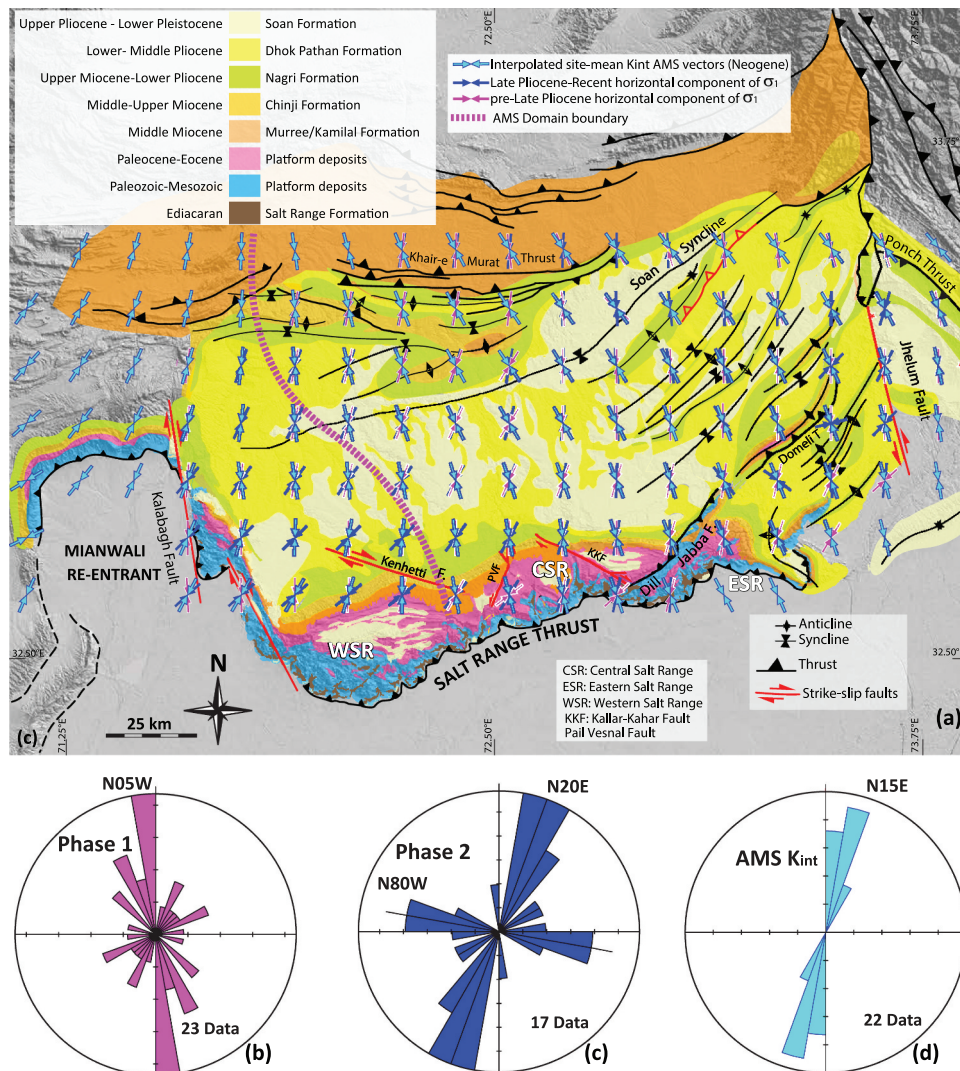


Figure 10. A) Horizontal components of major paleostress

(σ_1) axes for the first and the second phases of deformation superimposed with the horizontal component of the K_{int} axes. b-d) rose diagrams prepared from horizontal components of major paleostress (σ_1) and K_{int} orientations. Note the similarity between dominant σ_1 orientations (c) of phase 2 and K_{int} orientations (d).

orientation, especially in the western and northern parts of the thrust faults within the Potwar Plateau, such as Dill Jabba and Domeli, was interpreted as the indication of sliding the Potwar Plateau under the influence of gravity. Based on this interpretation, we hypothesize that Potwar Plateau has been translated southwards as a viscous fluid under the influence of gravity over the Neoproterozoic Salt Range Formation due to a slight compression exerted from the thrust faults to the north (Figure 11). Thus, the southward 'flow' of the plateau is possibly associated with a large number of minor faults observed extensively within the Salt Range.

The most prominent change in K_{int} orientations takes place in the western part of the Potwar Plateau. The area to the west of this boundary is controlled by the Kalabagh Fault in the west and Western Salt Range in the south. The thickness of the salt as a substratum in the eastern part of this domain boundary seems to be less compared to the western areas (Pennock *et al.* 1989).

The Potwar Plateau can be separated into two domains based on friction of the substratum. The salt decollement thins from west-to-east, and salt is completely absent farther to the east of the Dill Jabba fault. The presence of thick salt facilitates almost frictionless viscous flow within decollement, and overlying strata, and areas devoid of salt are affected by frictional

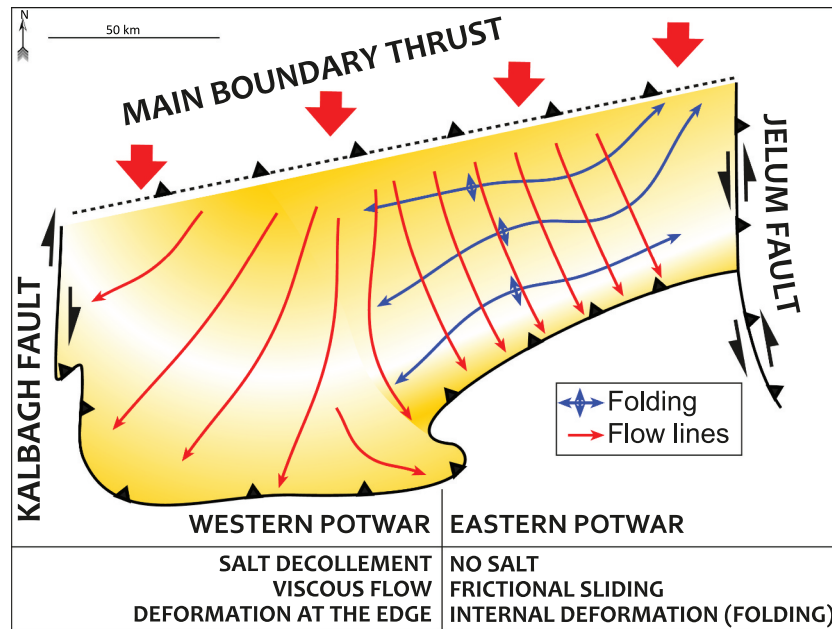


Figure 11. Simplified cartoon summarizing the main characteristics and deformation styles of different parts of Potwar Plateau.

sliding in the Potwar Plateau, as suggested by Borderie *et al.* (2018) based on analogue modelling. Such a change in thickness is reflected in the development of a series of folds in the east, while N-S directed compression and related shortening are taken up by Salt Range Thrust in the west, along the leading edge of the plateau (Figure 9). Thus, folding is the manifestation of the internal deformation of the eastern domains, and the lack of folding or internal contractional deformation in the western domains indicates that the deformation is taken up within the Salt Range Thrust that is associated with Ediacaran Salt horizons (Figure 11).

Almost the N-S orientation of the σ_1 axes associated with phase 1 and fanning out of σ_1 axes during the second phase of deformation indicates that proposed viscous and frictional deformation has been active at least since the Late Pliocene.

5. Conclusions

This study has reached the following main conclusions;

- (1) Two distinct deformation phases have been recognized in the Potwar Plateau.

The earlier deformation phase lasted until the Early Pliocene and was characterized by approximately horizontal N-S directed σ_1 and near-vertical σ_2 and σ_3 indicative of thrust tectonics.

The second deformation phase initiated in the Late Pliocene and has been active until recently. It is characterized by NNE-SSW directed compression and near-vertical intermediate principal stress (σ_2), indicative of transcurrent tectonics.

- (1) The interpolated σ_1 axes for the first deformation phase are almost parallel throughout the Potwar plateau, and they are interpreted as the indication of N-S directed orthogonal thrusting and shortening.
- (2) AMS data combined with the second deformation phase paleostress orientations indicate that the eastern and western half of the Potwar plateau can be subdivided kinematically into two major domains.
 - The western half is dominated by and lying above a salt decollement that facilitated viscous fluid-like deformation. Simultaneously, the N-S shortening has been taken up by the Salt Range thrust.
 - The eastern part of the plateau is completely (at the far east) or partially devoid of a salt substratum, promoting frictional deformation.
- (3) Interpolated σ_1 axes fan out from north to south-westwards for the second deformation phase, which is interpreted as the manifestation of unconstrained southwards gliding of the Potwar Plateau, over the Neoproterozoic salt, which

might have a higher thickness in the western part of the Potwar Plateau compared to the eastern part where there is no or very thin salt.

- The distribution of salt in the substratum is manifested by the dominance of NE-SW trending anticline-syncline pairs in the east and the absence of folds or thrusts in the western part of the Potwar Plateau.

Highlights

- AMS and Paleostress tensors elucidated Neogene kinematics of the Potwar Plateau.
- Two deformation phases controlled kinematics of the Potwar Plateau during the Neogene
- Western Potwar Plateau experiences low basal friction above the Precambrian salt décollement.
- Eastern Potwar Plateau experiences frictional sliding and internal deformation.
- Frictional and viscous flow mechanisms consume India-Eurasia convergence in the Potwar Plateau

Acknowledgments

We are thankful to the editor Robert Stern and the anonymous reviewers for their constructive comments that helped to improve the manuscript. We are also thankful to Asif Javed, Farooq Sultan and Syed Irfan Ali Zaidi for their help during fieldworks, valuable comments, and fruitful discussion. We are thankful for the logistic and administrative support provided by the Institute of Geology, University of the Punjab, Lahore Pakistan. This Study is part of AQ's PhD research at METU and Utrecht University. .

Disclosure of potential conflicts of interest

No potential conflict of interest was reported by the author(s).

Funding

This work was supported by the Utrecht University Visiting Research Fellow for NK ; AQ carried out his PhD research at METU and Utrecht University.

ORCID

Abdul Qayyum  <http://orcid.org/0000-0002-4731-8513>
 Nuretdin Kaymakci  <http://orcid.org/0000-0002-7618-0226>
 Cornelis G. Langereis  <http://orcid.org/0000-0001-9232-2178>
 Erhan Gülyüz  <http://orcid.org/0000-0002-1539-7982>
 Naveed Ahsan  <http://orcid.org/0000-0002-9468-126X>

References

Ahmad Abir, I., Khan, S.D., Ghulam, A., Tariq, S., and Shah, M.T., 2015, Active tectonics of western Potwar Plateau–Salt Range, northern Pakistan from InSAR observations and

- seismic imaging, *Remote Sensing of Environment*, 168 p. 265–275. [10.1016/j.rse.2015.07.011](https://doi.org/10.1016/j.rse.2015.07.011)
- Aleksandrowaski, P., 1985, Graphical determination of principal stress directions for slickenside lineation populations: An attempt to modify Arthaud's method, *J. Struct. Geol.*, 7, p. 73–82. [10.1016/0191-8141\(85\)90116-6](https://doi.org/10.1016/0191-8141(85)90116-6)
- Angelier, J., 1979, Determination of the mean principal directions of stresses for a given fault population, *Tectonophysics*, 56, [10.1016/0040-1951\(79\)90081-7](https://doi.org/10.1016/0040-1951(79)90081-7)
- Angelier, J., 1984, Tectonic analysis of fault slip data sets, *J. Geophys. Res.*, 89, p. 5835–5848. [10.1029/JB089iB07p05835](https://doi.org/10.1029/JB089iB07p05835)
- Angelier, J. 1994. Fault slip analysis and paleostress reconstruction. Hancock, N.L. ed. *Continental Deformation*. Pergamon Press: Oxford, 53–100.
- Armijo, R., Carey, E., and Cisternas, A., 1982, The inverse problem in microtectonics and the separation of tectonic phases, *Tectonophysics*, 82, p. 145–160. [10.1016/0040-1951\(82\)90092-0](https://doi.org/10.1016/0040-1951(82)90092-0)
- Aubourg, C., Rochette, P., and Vialon, P., 1990, Transport directions revealed by the magnetic fabric of sub-alpine terranoires (French Alps). *Comptes Rendus de l'Academie des Sciences Paris. Serie II*, 310 no.10, p. 1341–1346.
- Baker, D.M., Lillie, R.J., Yeats, R.S., Johnson, G.D., Yousuf, M., and Zamin, A.S.H., 1988, Development of the Himalayan frontal thrust zone: Salt Range, Pakistan, *Geology*, 16, p. 3–7. [10.1130/0091-7613\(1988\)016<0003:dotht>2.3.CO;2](https://doi.org/10.1130/0091-7613(1988)016<0003:dotht>2.3.CO;2)
- Borderie, S., Graveleau, F., Witt, C., and Vendeville, B.C., 2018, Impact of an interbedded viscous décollement on the structural and kinematic coupling in fold-and-thrust belts: Insights from analogue modeling, *Tectonophysics*, 722 p. 118–137. [10.1016/j.tecto.2017.10.019](https://doi.org/10.1016/j.tecto.2017.10.019)
- Borradaile, G.J., 2001, Magnetic fabrics and petrofabrics: Their orientation distributions and anisotropies, *Journal of Structural Geology*, 23, p. 1581–1596. [10.1016/S0191-8141\(01\)00019-0](https://doi.org/10.1016/S0191-8141(01)00019-0)
- Borradaile, G.J., and Henry, B., 1997, Tectonic applications of magnetic susceptibility and its anisotropy, *Earth-Science Reviews*, 42, p. 49–93. [10.1016/S0012-8252\(96\)00044-X](https://doi.org/10.1016/S0012-8252(96)00044-X)
- Borradaile, G.J., and Jackson, M., 2004, Anisotropy of magnetic susceptibility (AMS): Magnetic petrofabrics of deformed rocks, Geological Society, London, Special Publications, 238, p. 299–360. [10.1144/GSL.SP.2004.238.01.18](https://doi.org/10.1144/GSL.SP.2004.238.01.18)
- Bott, M.H.P., 1959, The Mechanics of Oblique Slip Faulting, *Geological Magazine*, 96 no.2, p. 109–117. [10.1017/S0016756800059987](https://doi.org/10.1017/S0016756800059987)
- Butler, R.W.H., 2018, Syn-kinematic strata influence the structural evolution of emergent fold – Thrust belts, *Geol. Soc. London, Spec. Publ.* 490. , [10.1144/SP490-2019-14](https://doi.org/10.1144/SP490-2019-14).
- Carey-Gailhardis, E., and Mercier, J.L., 1987, A numerical method for determining the state of stress using focal mechanisms of earthquake populations: Application to Tibetan teleseisms and microseismicity of Southern Peru, *Earth Planet. Sci. Lett.*, 82, p. 165–179. [10.1016/0012-821X\(87\)90117-8](https://doi.org/10.1016/0012-821X(87)90117-8)
- Chadima, M., & Jelinek, V. 2009. Anisoft 4.2: anisotropy data browser for windows. Agico.714 Inc, Brno.
- Chaudhry, M.N., and Ghazanfar, M., 1990, Position of the Main Central Thrust in the tectonic framework of Western Himalaya, *Tectonophysics*, 174, p. 321–329. [10.1016/0040-1951\(90\)90329-7](https://doi.org/10.1016/0040-1951(90)90329-7)

- Davis, D.M., and Engelder, T., 1985, The role of salt in fold-and-thrust belts, *Tectonophysics*, 119, p. 67–88. [10.1016/0040-1951\(85\)90033-2](https://doi.org/10.1016/0040-1951(85)90033-2)
- DeCelles, P.G., Robinson, D.M., Zandt, G., 2002, Implications of shortening in the Himalayan fold-thrust belt for uplift of the Tibetan Plateau, *Tectonics*, 21, p. 12-1-12–25. [10.1029/2001TC001322](https://doi.org/10.1029/2001TC001322)
- Delvaux, D., and Sperner, B., 2003, New aspects of tectonic stress inversion with reference to the TENSOR program. *Geol. Soc. London, Spec. Publ*, 212 p. 75–100. [10.1144/GSL.SP.2003.212.01.06](https://doi.org/10.1144/GSL.SP.2003.212.01.06)
- DiPietro, J.A., and Pogue, K.R., 2004, Tectonostratigraphic subdivisions of the Himalaya: A view from the west, *Tectonics*, 23, p. 1–20. [10.1029/2003TC001554](https://doi.org/10.1029/2003TC001554)
- Doblas, M., 1998, Slickenside kinematic indicators, *Tectonophysics*, 295 no.1–2, p. 187–197. [10.1016/S0040-1951\(98\)00120-6](https://doi.org/10.1016/S0040-1951(98)00120-6)
- Duermeijer, C.E., Van Vugt, N., Langereis, C.G., Meulenkaamp, J. E., and Zachariasse, W.J., 1998, A major late Tortonian rotation phase in the Croton basin using AMS as tectonic tilt correction and timing of the opening of the Tyrrhenian basin, *Tectonophysics*, 287, p. 233–249. [10.1016/S0040-1951\(98\)80071-1](https://doi.org/10.1016/S0040-1951(98)80071-1)
- Etchecopar, A., Vasseur, G., and Daignerier, M., 1981, An inverse problem in microtectonics for the determination of stress tensors from fault striation analysis, *Journal of Structural Geology*, 3, p. 51–65. [10.1016/0191-8141\(81\)90056-0](https://doi.org/10.1016/0191-8141(81)90056-0)
- Fleischmann, K.H., and Nemcok, M., 1991, Paleostress inversion of fault-slip data using the shear stress solution of Means (1989), *Tectonophysics*, 196, p. 195–202. [10.1016/0040-1951\(91\)90296-5](https://doi.org/10.1016/0040-1951(91)90296-5)
- Fleuty, M.J., 1974, Slickensides and slickenlines, *Geological Magazine*, 112, p. 319–322. [10.1017/S0016756800047087](https://doi.org/10.1017/S0016756800047087)
- Fleuty, M.J., 1975, Slickensides and slickenlines, *Geological Magazine*, 112, p. 319–322. [10.1017/S0016756800047087](https://doi.org/10.1017/S0016756800047087)
- Gee, E.R., 1989, Overview of the geology and structure of the Salt Range, with observations on related areas of Northern Pakistan, *Spec. Pap. Geol. Soc. Am*, 232 p. 95–112. [10.1130/SPE232-p95](https://doi.org/10.1130/SPE232-p95)
- Gephart, J.W., 1990, Stress and the direction of slip on fault planes, *Tectonics*, 9, p. 845–858. [10.1029/TC009i004p00845](https://doi.org/10.1029/TC009i004p00845)
- Gephart, J.W., and Forsyth, D.W., 1984, An improved method for determining the regional stress tensor using earthquake focal mechanism data: Application to the San Fernando Earthquake Sequence, *Journal of Geophysical Research*, 89, p. 9305–9320. [10.1029/JB089iB11p09305](https://doi.org/10.1029/JB089iB11p09305)
- Grelaud, S., Sassi, W., De Lamotte, D.F., Jaswal, T., and Roure, F., 2002, Kinematics of eastern Salt Range and South Potwar Basin (Pakistan): A new scenario, *Marine and Petroleum Geology*, 19, p. 1127–1139. [10.1016/S0264-8172\(02\)00121-6](https://doi.org/10.1016/S0264-8172(02)00121-6)
- Hancock, P.L., 1985, Brittle microtectonics: Principles and practice, *Journal of Structural Geology*, 7, p. 437–457. [10.1016/0191-8141\(85\)90048-3](https://doi.org/10.1016/0191-8141(85)90048-3)
- Hardcastle, K.C., 1989, Possible paleostress tensor configurations derived from fault-slip data in Eastern Vermont And Western New Hampshire, *Tectonics*, 8, p. 265–284. [10.1029/TC008i002p00265](https://doi.org/10.1029/TC008i002p00265)
- Hardcastle, K.C., and Hills, L.S., 1991, BRUTE3 and SELECT: QUICKBASIC 4 programs for determination of stress tensor configurations and separation of heterogeneous populations of fault-slip data, *Computers & Geosciences*, 17 no.1, p. 23–43. [10.1016/0098-3004\(91\)90078-R](https://doi.org/10.1016/0098-3004(91)90078-R)
- Henry, B., 1997, The magnetic zone axis: A new element of magnetic fabric for the interpretation of the magnetic lineation, *Tectonophysics*, 271, p. 325–331. [10.1016/S0040-1951\(96\)00267-3](https://doi.org/10.1016/S0040-1951(96)00267-3)
- Hirt, A.M., Lowrie, W., Clendenen, W.S., and Kligfield, R., 1993, Correlation of strain and the anisotropy of magnetic susceptibility in the Onaping Formation: Evidence for a near-circular origin of the Sudbury Basin, *Tectonophysics*, 225, p. 231–254. [10.1016/0040-1951\(93\)90300-9](https://doi.org/10.1016/0040-1951(93)90300-9)
- Hodges, K.V., 2000, Tectonics of the Himalaya and Southern Tibet from two perspectives, *Geological Society of America Bulletin*, 112, p. 324–350. [10.1130/0016-7606\(2000\)112<324:tothas>2.0.CO;2](https://doi.org/10.1130/0016-7606(2000)112<324:tothas>2.0.CO;2)
- Hrouda, F., 1982, Magnetic anisotropy of rocks and its application in geology and geophysics, *Geophysical Surveys*, 56, p. 37–82. [10.1016/0040-1951\(79\)90081-7](https://doi.org/10.1016/0040-1951(79)90081-7)
- Hrouda, F., and Janak, F., 1976, The changes in shape of the magnetic susceptibility ellipsoid during progressive metamorphism and deformation, *Tectonophysics*, 34, p. 135–148. [10.1016/0040-1951\(76\)90181-5](https://doi.org/10.1016/0040-1951(76)90181-5)
- Jackson, M., and Tauxe, L., 1991, Anisotropy of Magnetic Susceptibility and Remanence: Developments in the Characterization of Tectonic, Sedimentary and Igneous Fabric, *Reviews of Geophysics*, 89, p. 371–376. [10.1029/JB089iB07p05835](https://doi.org/10.1029/JB089iB07p05835)
- Jadoon, I.A.K., Hinderer, M., Wazir, B., Yousaf, R., Bahadar, S., Hassan, M., Abbasi, Z.-H., Jadoon, S., 2014, Structural styles, hydrocarbon prospects, and potential in the Salt Range and Potwar Plateau, north Pakistan, *Arab. J. Geosci*, 8, p. 5111–5125. [10.1007/s12517-014-1566-9](https://doi.org/10.1007/s12517-014-1566-9)
- Jadoon, I.A.K., Hinderer, M., Wazir, B., Yousaf, R., Bahadar, S., Hassan, M., Abbasi, Z.-U.-H., and Jadoon, S., 2015, Structural styles, hydrocarbon prospects, and potential in the Salt Range and Potwar Plateau, north Pakistan, . *Arabian Journal of Geosciences*, 8, p. 5111–5125. [10.1007/s12517-014-1566-9](https://doi.org/10.1007/s12517-014-1566-9)
- Jelinek, V., 1981, Characterization of the magnetic fabric of rocks, *Tectonophysics*, 79, p. 63–67. [10.1016/0040-1951\(81\)90110-4](https://doi.org/10.1016/0040-1951(81)90110-4)
- Jelínek, V., 1978, Statistical processing of anisotropy of magnetic susceptibility measured on groups of specimens, *Studia Geophysica Et Geodaetica*, 7, p. 50–62. [10.1016/0191-8141\(85\)90116-6](https://doi.org/10.1016/0191-8141(85)90116-6)
- Jouanne, F., 2014, Present-day deformation of northern Pakistan from Salt Ranges to Karakorum Ranges, *J. Geophys. Res. Solid Earth*, p. 1–17. [10.1002/2013JB010776](https://doi.org/10.1002/2013JB010776)
- Kapp, P., DeCelles, P.G., 2019, Mesozoic–Cenozoic geological evolution of the Himalayan-Tibetan orogen and working tectonic hypotheses, *Am. J. Sci*, 319, p.159–254. [10.2475/03.2019](https://doi.org/10.2475/03.2019)
- Kaymakci, N., White, S.H., and Van Dijk, P.M., 2000, Palaeostress Inversion in a Multiphase Deformed Area: Kinematic and Structural Evolution of the Çankırı Basin (Central Turkey), Part 1 – Northern Area. *Geological Society, London, Special Publications* 7, p. 295–323. [10.1016/0191-8141\(85\)90116-6](https://doi.org/10.1016/0191-8141(85)90116-6)
- Khan, S.D., Chen, L., Ahmad, S., Ahmad, I., and Ali, F., 2012, Lateral structural variation along the Kalabagh Fault Zone, NW Himalayan foreland fold-and-thrust belt, Pakistan,

- Journal of Asian Earth Sciences, 50 p. 79–87. [10.1016/j.jseas.2012.01.009](https://doi.org/10.1016/j.jseas.2012.01.009)
- Krantz, R.W., 1988, Multiple fault sets and three-dimensional strain: Theory and application, *Journal of Structural Geology*, 10, p. 225–237. [10.1016/0191-8141\(88\)90056-9](https://doi.org/10.1016/0191-8141(88)90056-9)
- Lacombe, O., 2010, Calcite Twins, a Tool for Tectonic Studies in Thrust Belts and Stable Orogenic Forelands, *Oil & Gas Science and Technology – Revue d'IFP Energies Nouvelles*, 65, p. 809–838. [10.2516/ogst/2009088](https://doi.org/10.2516/ogst/2009088)
- Lee, T.-Q., and Angelier, J., 2000, Tectonic significance of magnetic susceptibility fabrics in Plio-Quaternary mudstones of southwestern foothills, Taiwan, *Earth, Planets and Space*, 52, p. 527–538. [10.1186/BF03351660](https://doi.org/10.1186/BF03351660)
- Liesa, C.L., and Lisle, R.J., 2004, Reliability of methods to separate stress tensors from heterogeneous fault-slip data, *Journal of Structural Geology*, 26 no.3, p. 559–572. [10.1016/j.jsg.2003.08.010](https://doi.org/10.1016/j.jsg.2003.08.010)
- Lillie, R., 1987, Balanced Structural Cross Section of the Western Salt Range and Potwar Plateau. Pakistan: Deformation Near the Strike-Slip Terminus of an Overthrust Sheet. Oregon State University
- Marrett, R., and Allmendinger, R.W., 1990, Kinematic analysis of fault-slip data, *Journal of Structural Geology*, 12, p. 973–986. [10.1016/0191-8141\(90\)90093-E](https://doi.org/10.1016/0191-8141(90)90093-E)
- McDougall, J.W., Hussain, A., and Yeats, R.S., 1993, The Main Boundary Thrust and propagation of deformation into the foreland fold-and-thrust belt in northern Pakistan near the Indus River. *Geol. Soc. London, Spec. Publ.*, 74 p. 581–588. [10.1144/GSL.SP.1993.074.01.38](https://doi.org/10.1144/GSL.SP.1993.074.01.38)
- Meade, B.J., 2007, Present-day kinematics at the India-Asia collision zone, *Geology*, 35, p. 81–84. [10.1130/G22924A.1](https://doi.org/10.1130/G22924A.1)
- Means, W.D., 1976, *Stress and strain*. Springer-Verlag New York Heidelberg Berlin, 342p.
- Molnar, P., and Tapponnier, P., 1978, Active Tectonics Of Tibet, *Journal of Geophysical Research*, 83, p. 5361–5375. [10.1029/JB083iB11p05361](https://doi.org/10.1029/JB083iB11p05361)
- Najman, Y., Appel, E., Fadel, M.B., Bown, P., Carter, A., Garzanti, E., Godin, L., Han, J., Liebke, U., Oliver, G., Parrish, R., and Vezzoli, G., 2010, Timing of India-Asia collision: Geological, biostratigraphic, and palaeomagnetic constraints, *Journal of Geophysical Research*, 115, p. 1–18. [10.1029/2010JB007673](https://doi.org/10.1029/2010JB007673)
- Nieto-Samaniego, A.F., and Alaniz-Alvarez, S.A., 1997, Origin and tectonic interpretation of multiple fault patterns, *Tectonophysics*, 270, p. 197–206. [10.1016/S0040-1951\(96\)00216-8](https://doi.org/10.1016/S0040-1951(96)00216-8)
- Opdyke, N.D., and Lindsay, E., 1979, Magnetic polarity stratigraphy and vertebrate paleontology of the upper siwalik subgroup of northern Pakistan, *Palaeogeography, Palaeoclimatology, Palaeoecology*, 27 p. 1–34. [10.1016/0031-0182\(79\)90091-9](https://doi.org/10.1016/0031-0182(79)90091-9)
- Pares, J.M., and Van Der, B.A., 2002, Evaluating magnetic lineations (AMS) in deformed rocks, *Tectonophysics*, 350, p. 283–298. [10.1016/S0040-1951\(02\)00119-1](https://doi.org/10.1016/S0040-1951(02)00119-1)
- Pennock, E.S., Lillie, R.J., Zaman, A.S.H., and Yousaf, M., 1989, Structural interpretation of seismic reflection data from the eastern salt range and potwar plateau, Pakistan, *Am. Assoc. Pet. Geol. Bull.*, 73 p. 841–857. [10.1306/44B4A27B-170A-11D7-8645000102C1865D](https://doi.org/10.1306/44B4A27B-170A-11D7-8645000102C1865D)
- Qayyum, M., Spratt, D.A., Dixon, J.M., and Lawrence, R.D., 2015, Displacement transfer from fault-bend to fault-propagation fold geometry: An example from the Himalayan thrust front, *Journal of Structural Geology*, 77 p. 260–276. [10.1016/j.jsg.2014.10.010](https://doi.org/10.1016/j.jsg.2014.10.010)
- Reches, Z., 1987, Determination of the tectonic stress tensor from slip along faults that obey the coulomb yield condition, *Tectonics*, 6, p. 849–861. [10.1029/TC006i006p00849](https://doi.org/10.1029/TC006i006p00849)
- Rochette, P., Jackson, M., and Aubourg, C., 1992, Rock magnetism and the interpretation of Anisotropy of Magnetic Susceptibility, *Reviews of Geophysics*, 30 no.3, p. 209–226.
- Sagnotti, L., and Speranza, F., 1993, Magnetic fabric analysis of the Plio-Pleistocene clayey units of the Sant'Arcangelo basin, southern Italy, *Physics of the Earth and Planetary Interiors*, 77, p. 165–176. [10.1016/0031-9201\(93\)90096-R](https://doi.org/10.1016/0031-9201(93)90096-R)
- Studýnka, J., Chadima, M., and Suza, P., 2014, Fully automated measurement of anisotropy of magnetic susceptibility using 3D rotator, *Tectonophysics*, 629 p. 6–13. [10.1016/j.tecto.2014.02.015](https://doi.org/10.1016/j.tecto.2014.02.015)
- Tapponnier, P., Peltzer, G., and Armijo, R., 1986, On the mechanics of the collision between India and Asia. *Geol. Soc. London, Spec. Publ.*, 19 p. 113–157. [10.1144/GSL.SP.1986.019.01.07](https://doi.org/10.1144/GSL.SP.1986.019.01.07)
- Tauxe, L., and Feakins, S.J., 2020, A Reassessment of the Chronostratigraphy of Late Miocene C 3 –C4 Transitions, *Paleoceanography and Paleoclimatology*, 35(7), p. e2020PA003857.35no. 7, [10.1029/2020PA003857](https://doi.org/10.1029/2020PA003857).
- Wallace, R.E., 1951, The geometry of Shearing Stress and Relation to Faulting, *The Journal of Geology*, 59, p. 118–130. [10.1086/625831](https://doi.org/10.1086/625831)
- Will, T.M., and Powell, R., 1991, A robust approach to the calculation of paleostress fields from fault plane data, *Journal of Structural Geology*, 13, p. 813–821. [10.1016/0191-8141\(91\)90006-5](https://doi.org/10.1016/0191-8141(91)90006-5)
- Yeats, R.S., and Hussain, A., 1987, Timing of structural events in the Himalayan foothills of northwestern Pakistan, *Geological Society of America Bulletin*, 99, p. 161–176. [10.1130/0016-7606\(1987\)99<161:TOSEIT>2.0.CO;2](https://doi.org/10.1130/0016-7606(1987)99<161:TOSEIT>2.0.CO;2)
- Yeats, R.S., Khan, S.H., and Akhtar, M., 1984, Late Quaternary deformation of the Salt Range of Pakistan, *Geological Society of America Bulletin*, 95, p. 958–966. [10.1130/0016-7606\(1984\)95<958:lqdots>2.0.CO;2](https://doi.org/10.1130/0016-7606(1984)95<958:lqdots>2.0.CO;2)
- Yeats, R.S., Nakata, T., Farah, A., Front, M., Mirza, M.A., Panday, M., and Stein, R., 1992, The Himalayan Frontal System, *Ann. Tectonics Spec*, 6, p. 85–86.
- Yeats, R.S., and Thakur, V.C., 2008, Active faulting south of the Himalayan Front: Establishing a new plate boundary, *Tectonophysics*, 453, p. 63–73. [10.1016/j.tecto.2007.06.017](https://doi.org/10.1016/j.tecto.2007.06.017)
- Žalohar, J., and Vrabec, M., 2007, Paleostress analysis of heterogeneous fault-slip data: The Gauss method, *Journal of Structural Geology*, 29 no.11, p. 1798–1810. [10.1016/j.jsg.2007.06.009](https://doi.org/10.1016/j.jsg.2007.06.009)
- Yin, Z.M., Ranalli, G., 1993, Determination of tectonic stress field from fault slip data: Toward a probabilistic model, *J. Geophys. Res.*, 98, p. 12165–12176. <https://doi.org/10.1029/93jb00194>